

Density and temperature dependence of production rates of ${}^6\text{He}$, ${}^9\text{Be}$, ${}^{12}\text{C}$

D.V. Fedorov*

Aarhus University, Aarhus, Denmark

R. de Diego

Instituto de Estructura de la Materia, Madrid, Spain

E. Garrido

Instituto de Estructura de la Materia, Madrid, Spain

A.S. Jensen

Aarhus University, Aarhus, Denmark

We consider dense and hot environments consisting of α -particles and neutrons. These environments possibly appear after type II supernova explosions and are the suggested starting place for the rapid-neutron process. Three nucleosynthesis reactions are possible in such environments, $3\alpha \rightarrow {}^{12}\text{C} + \gamma$, $2\alpha + n \rightarrow {}^9\text{Be} + \gamma$, and $\alpha + 2n \rightarrow {}^6\text{He} + \gamma$, all of which are three-body reactions. We investigate the reaction rates of these reactions as function of the density and the temperature of the environment. We use genuine three-body models without sequential approximation.

11th Symposium on Nuclei in the Cosmos, NIC XI

July 19-23, 2010

Heidelberg, Germany

*Speaker.

1. Introduction

In neutron-rich scenarios of astrophysical nucleosynthesis heavy elements are formed by the rapid neutron process in hot and dense environments consisting of α -particles and neutrons [1]. Formation of heavy elements must overcome the problem that all nuclear isotopes with mass numbers 5 and 8 are unstable [2]. These gaps can be bridged by the three-body reactions

$$\alpha + \alpha + \alpha \rightarrow {}^{12}\text{C} + \gamma, \quad (1.1)$$

$$\alpha + \alpha + n \rightarrow {}^9\text{Be} + \gamma, \quad (1.2)$$

$$\alpha + n + n \rightarrow {}^6\text{He} + \gamma. \quad (1.3)$$

These three-body reactions are usually treated as two-step processes where the unstable isotopes ${}^5\text{He}$ and ${}^8\text{Be}$ are first created, which subsequently, before decaying, react with another neutron or α -particle [3, 4, 5]. This approximation of two independent sequential processes does not always provide an accurate description, in particular in cases when the lifetimes of the intermediate configurations are comparable to, or shorter than, the reaction time of the last step of the process [6]. This implies that these processes proceed through genuine three-body reactions.

The purpose of this contribution is to investigate the relative production rates of the three possible reactions as function of the density and the temperature of the environment, using the genuine three-body reaction dynamics without sequential approximation.

2. Production rates

The rate $R_{abc}(E)$ of the radioactive capture reaction $a + b + c \rightarrow A + \gamma$ from a continuum state of particles a, b, c with kinetic energy E can be related to the cross-section of the inverse photo-dissociation reaction [7],

$$R_{abc}(E) = \frac{\hbar^3}{c^2} \frac{8\pi}{(\mu_x \mu_y)^{3/2}} \left(\frac{E_\gamma}{E} \right)^2 \frac{2g_A}{g_a g_b g_c} \sigma_\gamma(E_\gamma), \quad (2.1)$$

where $E = E_\gamma + B_A$ is the kinetic energy of the initial continuum three-body state, E_γ is the photon energy, $\sigma_\gamma(E_\gamma)$ is the photo-dissociation cross-section of the nucleus A , c is the speed of light, g_i is the degeneracy of particles $i = a, b, c, A$, and μ_x and μ_y are the reduced masses of the systems related to the Jacobi coordinates, (\mathbf{x}, \mathbf{y}) , for the three-body system [8].

The photo-dissociation cross-section for the inverse process $A + \gamma \rightarrow a + b + c$ can be expanded into electric and magnetic multipoles. In particular, the electric multipole contribution of order λ has the form [9]

$$\sigma_\gamma^{(\lambda)}(E_\gamma) = \frac{(2\pi)^3 (\lambda + 1)}{\lambda [(2\lambda + 1)!!]^2} \left(\frac{E_\gamma}{\hbar c} \right)^{2\lambda - 1} \frac{d\mathcal{B}}{dE}, \quad (2.2)$$

where the strength function \mathcal{B} is

$$\mathcal{B}(E\lambda, n_0 J_0 \rightarrow nJ) = \sum_{\mu M} |\langle nJM | O_\mu^\lambda | n_0 J_0 M_0 \rangle|^2, \quad (2.3)$$

where J_0 , J and M_0 , M are the total angular momenta and their projections of the initial and final states, and all the other quantum numbers are collected into n_0 and n . The electric multipole operator is given by

$$O_\mu^\lambda = \sum_{i=1}^3 z_i |\mathbf{r}_i - \mathbf{R}|^\lambda Y_{\lambda,\mu}(\Omega_{y_i}), \quad (2.4)$$

where i runs over the three particles, and where we neglect contributions from intrinsic transitions within each of the three constituents [10].

The strength function, \mathcal{B} , is computed by genuine three-body calculations of both the bound final state and the continuum initial states. We use the hyper-spherical adiabatic expansion method described in [8]. The n - n , α - n , and α - α interactions are given in [11, 12]. The continuum three-body states of given angular momentum and parity are calculated using the box boundary conditions [13]. The continuum spectrum is thus discretized. The strength functions are then calculated for each discrete continuum state using (2.3). The distribution $d\mathcal{B}/dE$ is built using the finite energy interval approximation, where the energy range is divided into bins, and all the discrete values of \mathcal{B} falling into a given bin are summed up. Afterwards the points are connected by splines and the expressions (2.2) and (2.5) are computed.

2.1 Temperature and density dependence

The production rate $P_{abc}(\rho, T)$ of a recombination reaction as function of the density ρ and temperature T of the environment is obtained by averaging $R_{abc}(E)$ with the Maxwell-Boltzmann distribution over the initial energies E and multiplying by the density n_i of particles a , b , and c . These densities are usually written as $n_i = \rho N_A X_i / A_i$, where ρ is the density of the environment, N_A is the Avogadro's number, A_i is the mass number of particle i , and $X_i = N_i M_i / (N_a M_a + N_b M_b + N_c M_c)$ is the mass abundance of nucleus i expressed by the number of particles N_i and their masses M_i (see Eqs.(1) and (3) in ([7]),

$$P_{abc}(\rho, T) = n_a n_b n_c \frac{\hbar^3}{c^2} \frac{8\pi}{(\mu_x \mu_y)^{3/2}} \frac{g_A}{g_a g_b g_c} e^{-\frac{B}{k_B T}} \frac{1}{(k_B T)^3} \int_{|B|}^{\infty} E_\gamma^2 \sigma_\gamma(E_\gamma) e^{-\frac{E_\gamma}{k_B T}} dE_\gamma. \quad (2.5)$$

It is also possible to use the relative abundance $Y_i = N_i / (N_a + N_b + N_c)$.

The density dependence of the production rates (2.5) is very simple for a given temperature – the reaction rate for three particles has to be multiplied by the number of each species of particles. For a given total density ρ which is the sum of the neutron and α -particle densities, the density dependence is given as $\rho^3 X_\alpha^n X_n^{3-n}$, where $X_n = 1 - X_\alpha$ and X_α are the mass fraction of neutrons and α -particles. Then $n = 1, 2, 3$ corresponds to production of ${}^6\text{He}$, ${}^9\text{Be}$ and ${}^{12}\text{C}$, respectively.

When no α -particles are present, $X_\alpha = Y_\alpha = 0$, the production rates are all zero. When only α -particles are present, $X_\alpha = Y_\alpha = 1$, only ${}^{12}\text{C}$ can be produced. The density dependence for production of ${}^6\text{He}$ and ${}^9\text{Be}$ are each others reflection against $X_\alpha = 1/2$ but are pushed toward smaller values as function of Y_α . The production of ${}^{12}\text{C}$ increases monotonically as function of X_α and Y_α .

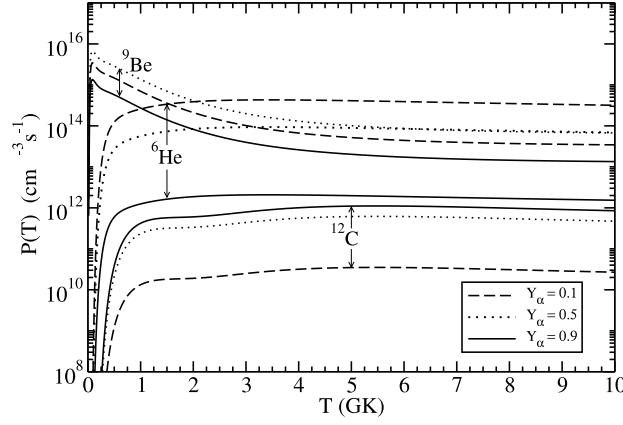


Figure 1: Production rates of ${}^6\text{He}$, ${}^9\text{Be}$, and ${}^{12}\text{C}$ as function of temperature for several densities.

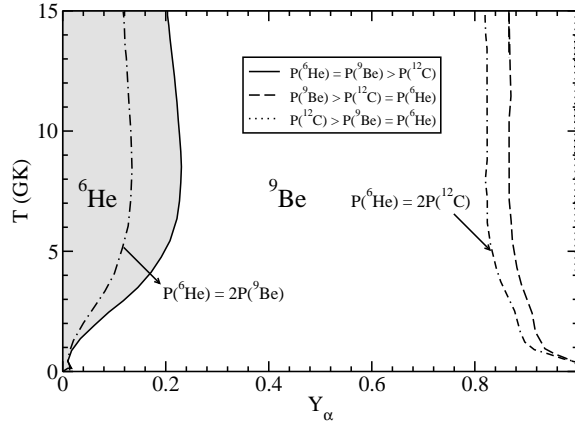


Figure 2: The phase diagram for production ${}^6\text{He}$, ${}^9\text{Be}$ and ${}^{12}\text{C}$ in the Y_α - T parameter space. The curves correspond to a constant ratio of production rates of two nuclei.

3. Relative production yields

We show in fig.1 the average rates as function of temperature for several densities. All important contributions from different angular momenta and parities, or equivalently different electromagnetic transitions, are included in the figure. We see that ${}^{12}\text{C}$ is very low, but of course increasing relatively with alpha-particle abundance. At higher temperature the ${}^6\text{He}$ contributions dominate whereas ${}^9\text{Be}$ by far has the largest contribution at very low temperature. Responsible for the ${}^9\text{Be}$ dominance is the $1/2+$ state which is above but very close to ${}^8\text{Be}(0+)$ threshold [14].

The complete picture of the density-temperature dependence of the three-body production rates is shown in fig.2. All these nuclei can be destroyed in the same environment but we consider here only the individual three-body reactions creating them. Transfer reactions from ${}^6\text{He}$ and ${}^9\text{Be}$ using the same basic ingredients of neutrons and alphas can also produce ${}^9\text{Be}$ and ${}^{12}\text{C}$. Again, these nuclei can be produced in four-body recombination reactions[15]. However, all these processes are beyond the scope of the present investigation. For Y_α less than about 0.1 and temperatures above $T \approx 1 - 4$ GK the nucleus ${}^6\text{He}$ is produced more than twice as often as ${}^9\text{Be}$. As Y_α increases the relative ${}^9\text{Be}$ production increases and becomes dominant for all temperatures when Y_α exceeds 0.2.

The rates at very low temperatures are difficult to estimate numerically as they require extrapolation to zero energy which in turn require certain assumptions about the asymptotic behavior of the photo-dissociation cross-section[16].

By further increase of Y_α the relative creation rate of ${}^{12}\text{C}$ increases. At $Y_\alpha \approx 0.82$ the ${}^9\text{Be}$ production is still dominating when ${}^{12}\text{C}$ is created with half the rate of ${}^6\text{He}$. At $Y_\alpha \approx 0.86$ the production rates for ${}^{12}\text{C}$ and ${}^6\text{He}$ are equal, but the production of ${}^9\text{Be}$ still dominates. Only when Y_α is larger than about 0.99, where very few neutrons are present, the production rate of ${}^{12}\text{C}$ exceeds the other rates. These relative rates are very crudely independent of temperature except for very low Y_α values. Except for the small Y_α results, similar overall conclusions were obtained in previous investigations [3, 17, 18].

References

- [1] B.S. Meyer G.J. Mathews, W.M. Howard, S.E. Woosley, and R.D. Hoffman, *Astrophys. J.* 399, 656 (1992).
- [2] A. Aprahamian, K. Langanke, M. Wiescher, *Prog. Part. Nucl. Phys.* 54, 535 (2005).
- [3] V.D. Efros, W. Balogh, H. Herndl, R. Hofinger, and H. Oberhummer, *Z. Phys. A* 355, 101 (1996).
- [4] K. Sumiyoshi, H. Utsunomiya, S. Goko, and T. Kajino, *Nucl. Phys. A* 709, 467 (2002).
- [5] A. Bartlett, J. Görres, G.J. Mathews, K. Otsuki, M. Wiescher, D. Frekers, A. Mengoni, and J. Tostevin, *Phys. Rev. C* 74, 015802 (2006).
- [6] H.O.U. Fynbo, R. Álvarez-Rodríguez, A.S. Jensen, O.S. Kirsebom, D.V. Fedorov, E. Garrido, *Phys. Rev. C* 79, 054009 (2009).
- [7] W. A. Fowler, G. R. Caughlan, and B. A. Zimmerman, *Annu. Rev. Astron. Astrophys.* 5, 525 (1967).
- [8] E. Nielsen, D.V. Fedorov, A.S. Jensen, and E. Garrido, *Phys. Rep.* 347, 373 (2001).
- [9] C. Forseén, N.B. Shul'gina, M.V. Zhukov, *Phys. Rev. C* 67, 045801 (2003).
- [10] C. Romero-Redondo, E. Garrido, D.V. Fedorov, and A.S. Jensen, *Phys. Rev. C* 77, 054313 (2008).
- [11] R. Alvarez-Rodriguez, E. Garrido, A.S. Jensen, D.V. Fedorov, and H.O.U. Fynbo, *Eur.Phys.J. A* 31, 303 (2007).
- [12] E. Garrido, D.V. Fedorov, A.S. Jensen, *Nucl. Phys. A* 700, 117 (2002).
- [13] R. de Diego, E. Garrido, D.V. Fedorov, A.S. Jensen, *Phys. Rev. C* 77, 024001 (2008).
- [14] E. Garrido, D.V. Fedorov, and A.S. Jensen, *Physics Letters B*, 684, 123 (2010).
- [15] R. de Diego, E. Garrido, D.V. Fedorov, A.S. Jensen, *Journal of Physics G*, to be published.
- [16] E. Garrido, D.V. Fedorov, A.S. Jensen, to be published.
- [17] V.D. Efros, H. Oberhummer, A. Puskhin, I.J. Thompson *Eur. Phys. J. A* 1, 447 (1998).
- [18] J. Görres, H. Herndl, I.J. Thompson, M. Wiescher, *Phys. Rev. C* 52, 2231 (1995).